High Gain Avalanche Photodiode Arrays for DIRC Applications[1]

S. Vasile[2], R. J. Wilson[3], S. Shera[2], D. Shamo[2], M.R. Squillante[2]

[2]Radiation Monitoring Devices, Inc. Watertown, Massachusetts 02472

[3]Colorado State University, Fort Collins, Colorado 80523

Abstract

The detection of light emitted in Cherenkov radiators requires fast detector arrays with high sensitivity to short wavelength photons. Photomultiplier tubes, the traditional imaging detectors for short wavelength optical radiation, have limited spatial resolution and require expensive anti-magnetic shielding.

We report on the performance of a new, Geiger mode operated, silicon micro-avalanche photodiode (?APD) array, designed for Cherenkov light imaging applications. We address issues of optical interfacing, speed, and pulse spectra achievable with these ?APDs.

The new ?APD array provides a high sensitivity detector for applications requiring two dimensional light mapping with single photon sensitivity. These features make it a promising candidate for the detection of Cherenkov light in modern high energy physics experiments.

I. INTRODUCTION

The Cherenkov detector is an excellent tool for energetic charged particle identification in high-energy and nuclear physics experiments. A low number of blue/near-UV photons is generated in Cherenkov radiators. High sensitivity optical sensors, combining single photon counting with information on the spatial distribution of incoming photons are needed for the new generation of Cherenkov detectors.

An excellent charged particle identification system is essential at the new PEP-II asymmetric e^+e^- collider facility at Stanford Linear Accelerator Center (SLAC). A new type of imaging Cherenkov detector, Detection of Internally Reflected Cherenkov light (DIRC) has been developed for this facility [1]. The compact and low radiation-length design of this detector allow the surrounding calorimeter to be smaller, at considerable cost saving, and produces less energy degradation than other ring-imaging devices. The detector has been engineered to be read-out with 10,752 photomultiplier tubes (PMT).

PMTs and PMT arrays have progressed towards miniaturization and low cost with the availability of multi-anode devices. However, for single photon applications, some of the remaining limitations are: susceptibility to magnetic fields, limited number of pixels per array due to electrostatic limitations, gain stability, and the need for stable threshold discriminators unless signal post-amplification is implemented. The angular resolution needed for accurate Cherenkov cone angle reconstruction requires that these relatively large PMTs must be positioned far from the quartz radiator bars. This results in a 4 m diameter imaging system and a tank containing 6 tons of pure water, acting as refractive index matching medium between the radiator bars and the PMTs. Small area optical detectors, with performance comparable or exceeding the PMT's sensitivity, gain and speed, would allow compact, high angular resolution readouts.

Current silicon technology allows the fabrication of optical imaging arrays with high resolution and large number of pixels, at affordable cost. Silicon APDs are **p-n** junction, solid state detectors with high internal gain. When biased above the breakdown voltage (Geiger mode) they can detect single photons and generate pulses with amplitudes of 1-4 V. Due to the short electrical carrier paths and their planar structure, APDs have an intrinsic high immunity to magnetic fields.

In a previous paper, we reported on the performance of novel ?APD arrays with single photon detectivity at room temperature, improved UV sensitivity and gain in the $10^8 - 10^9$ range [2]. During the last year, we have investigated the feasibility of utilizing these ?APD arrays as readout detectors for DIRC type designs. In this paper we will report on the design of ?APD optical interfacing with the DIRC radiators, pulse signal spectra, and improvements on speed.

II. DIRC OPTICAL INTERFACING WITH ?APDs

A. Light Generation in Quartz Radiators

DIRC is a ring imaging Cherenkov detector based on total internal reflection and uses long, rectangular bars made from

synthetic fused quartz as both radiator medium and light guides. The detector is thin, fast, robust, and is designed to tolerate high background radiation levels. A charged particle, traversing the quartz radiators, produces a Cherenkov light cone if its velocity is greater than the velocity of light in that medium. The opening angle of this cone is directly related to the particle velocity. Some part of the Cherenkov radiation is captured by internal reflection in the bar and is transmitted to the photon detector array, located at one of the radiator ends. The optical quality of the quartz radiators preserves the angle of the emitted Cherenkov light. The measurement of this angle, in conjunction with the measurement of the track angle and particle momentum, allows the determination of the particle mass. The light cone image is usually detected with PMT arrays situated at more than 1m distance from the quartz radiator end. To provide an alternative approach to the PMT design, we are developing new APD arrays capable of imaging the Cherenkov light in close proximity to the quartz bar end. We chose to use the focusing mirror geometry (focusing DIRC) to confine the Cherenkov image to a much smaller size [3].

B. Optical Interfacing with DIRC radiator

This geometry uses a cylindrical or spherical mirror to focus the Cherenkov light cone back onto a focal plane situated above the quartz radiator (see Figure 1). We use a focusing mirror (solid quartz block coated with Aluminum or another high UV-reflectivity material) mounted directly onto the end of the radiator to maximize optical transmission to the photodetector. The UV-reflective surface focuses the rays, emerging at the same angle from the quartz radiator, onto an array of mirror concentrators optically coupled to the ?APD array pixels. These light concentrators are also coated with high reflectivity materials, so that the rays propagate through quartz until they reach the APD pixel.
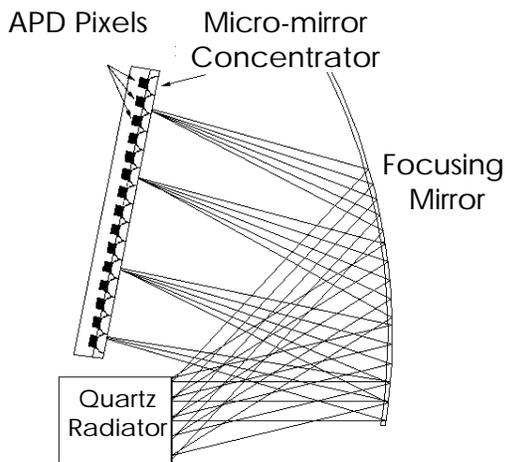

Figure 1: Two-dimensional ray tracing of the optical interface between the quartz radiator and ?APD array. A quartz radiator with 1.8 cm vertical dimension, matching the size of DIRC radiators at the BaBar detector [SLAC] was used in the ray tracing geometry. The

mirror transforms the image from the Cherenkov cone angle domain into the space domain. The rays are focused onto a tilted image plane. As all rays propagate in the quartz medium only, no total internal reflection at the quartz radiator exit surface occurs. The rays are further concentrated onto the active area of the APD pixels using silica micro-mirror concentrators with 300 ?m pitch size. Rays are traced for 0, 15, 26 and 47? exit angle from the quartz radiator.

The imaging plane (concentrator array plane) angle is optimized to minimize the maximum ray incidence angle. For this particular design, the maximum ray incidence half-angle is 17?. Three-dimensional ray tracing results (using BEAM 3 by Stellar Software) show that, for this maximum incidence angle, more than 70% of the photons reaching the mirror concentrator will be focused onto the ?APD sensitive area, if a 4:1 area ratio concentrator is used. The use of mirror concentrators will result in a fill factors close to 100%, will minimize the ?APD sensitive area, and consequently the dark count rate (noise). The maximum distance from the quartz radiator to the cylindrical mirror is approximately 5 cm, as opposed to 117 cm encountered in the present DIRC designs using PMT arrays. Therefore, designs using ?APDs would result in more compact hardware, would simplify the engineering solutions, and could result in significantly lower system cost.

C. APD Array Layout

The prototype ?APD array was designed to have 6 x 14 pixels with 300 ?m pitch size. The ?APD array has a common anode row and redundant connections at both ends of the array (see Figure 2). We are currently fabricating the array on 5" silicon wafers.
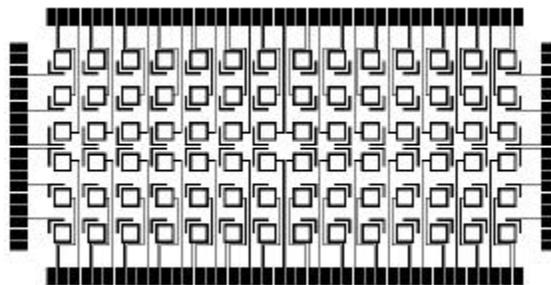

Figure 2: Layout of the interconnection layer for 6 x 14 pixels ?APD array. All pixels in a row will have the anodes connected to the lateral pads (row isolation). The cathodes of each APD are wired to the pads lined on the long sides of the rectangle. The pitch size is 300 ?m and the APD active area is 150 ?m x 150 ?m.

III. APD ACTIVE QUENCHING

Geiger mode operated APDs exhibit gains as high as 10^8. In this configuration an avalanche current pulse is triggered either by a photo-generated carrier or by a thermally generated carrier. Conventional operation of the APD in Geiger mode is accomplished by biasing the device above the breakdown voltage and leaving the external bias permanently connected to the device through a limiting resistor (passive quenching).

Once the avalanche is initiated, the charge carriers generated by the avalanche process are swept through the diode structure by the applied field, gradually depleting the capacitance of the device. As the field collapses due to the voltage drop on the current limiting resistor, the acceleration of free carriers is brought to an end and the avalanche is quenched. The Geiger event reset time in passive quenching mode is in the 10-30 ?sec range (see Figure 3).
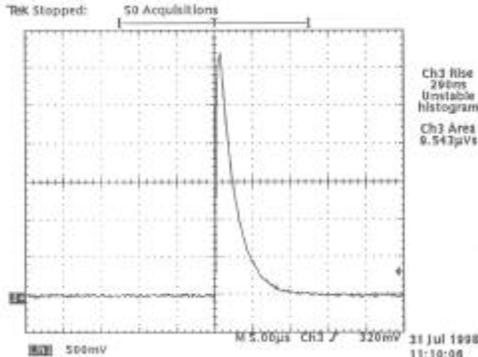

Figure 3: Geiger pulse shape for passive quenching with a limiting (quenching) resistor (horizontal scale 5 ?sec/div, vertical scale 500mV/div, bias 45.5 volts). The peak current pulse is 33 ?A and the corresponding gain is 5 x 10^8.

A. Active Quenching with Comparators

In order to overcome the limitations of the passive quenching scheme, active quenching circuits have been investigated for several years [4-6]. In the active quenching mode, the leading edge of passively quenched Geiger pulse triggers a fast comparator to initiate the quenching and recharging processes. Figure 4 shows the early leading edge of a Geiger pulse generated in ?APD. The slew rate is approximately 30 V/?sec. We expect low time jitter contribution of the ?APD to the overall active quenching circuit timing performance, as the measured rise time fluctuations on our ?APDs is less than 250 psec [7].
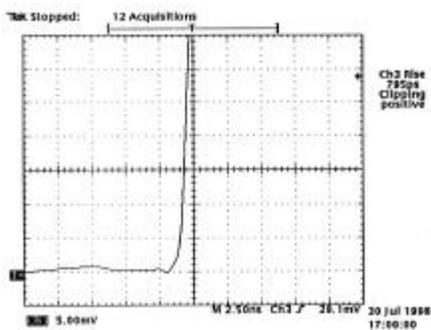

Figure 4: Leading edge of the Geiger pulse for 100 K? limiting resistor (horizontal scale 2.5 nsec/div, vertical scale 5 mV/div). The slew rate is approximately 30 V/?sec. Low threshold detection (30 mV) may result in less than 2 nsec time delay.

Figure 5 presents the conceptual schematic of an active quenching circuit design. In this system, a discriminator detects the ?APD Geiger signal. The discriminator output drives a fast solid state switching device used to decrease the avalanche diode bias below breakdown (quench). The MOS quench transistor also provides a low impedance path, thus resulting in fast discharge time. After the avalanche is quenched and the Geiger charge is drained to ground, the voltage is increased above breakdown and the ?APD is ready for the next event detection.
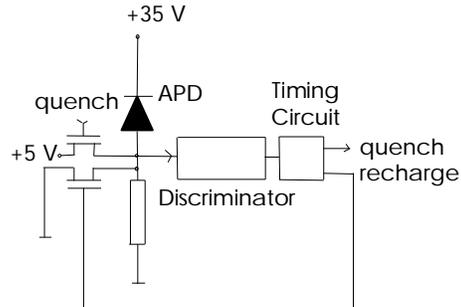

Figure 5: Active circuit configuration.

An active quenching circuit was fabricated at RMD using the configuration shown in Figure 5 [8] and the original design developed at SSC [9]. The circuit detects the leading edge of the passively quenched pulse using a fast comparator. A tri-state circuit decreases the voltage on the ?APD (high state, low impedance) and effectively quenches the avalanche. Reset timing is provided by an RC delay. Geiger pulses, generated in ?APD and quenched with the active quenching scheme, are shown in Figure 6. The active quenching circuit used an AD9696 fast comparator. Because the comparator sinks currents larger than the ?APD Geiger pulse current, the bias above the breakdown voltage cannot exceed 2.5V, thus limiting the device sensitivity (the ?APD reaches optimum sensitivity at approximately 4 V above the breakdown voltage).
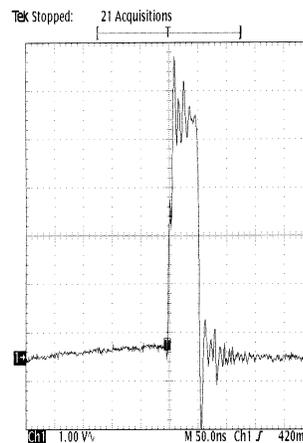

851

Figure 6: Actively quenched pulse for 20 ?m diameter ?APDs. The comparator switches at 200 mV and generates a 50 nsec wide pulse with 5 nsec rise and fall time. (horizontal scale 50nsec/div, vertical scale 1V/div).

In order to overcome the limitations in sensitivity, low input current comparators were tested. We fabricated and tested the active quenching circuit performance using MAX913 (Maxim) comparators. Functional tests were performed for each of the above designs, the timing performance in terms of rise time, fall time and pulse width was evaluated and the conclusions summarized in Table I. The stability of the active quenching circuit has been improved by using MAX913. However due to longer transit time, the pulse width increased from 50 to 70 nsec.

Table I. Active circuit timing performance for two fast comparators. MAX 913 has superior performance in terms of stability and lower total bias current (5 ? A as compared to 50 ? A for AD9696).

Comparator	Input current	Propagation Delay	Rise Time	Fall Time	Pulse Width
	? A	nsec	nsec	nsec	nsec
AD9696	50	2.5	7	7	50
MAX913	5	10	5	8	70

B. Pulsed Quenching

The integration of active quenching schemes using comparators requires many active components per pixel and is unlikely to be used for large size ?APD arrays. We tested an alternative active quenching scheme requiring a minimal number of components / pixel, with the goal of integrating simple active quenching circuitry on large size ?APD arrays. We investigated the pulsed bias quenching, consisting of fast, high amplitude pulses (60 - 70 V) applied to the ?APD through a limiting resistor (Figure 7a). Such a circuit allows fast quenching, but results in approximately 500 nsec reset time. This slow recovery is attributed to the relatively high impedance of the ?APD junction controlling the charge drain at the end of the pulsed bias. Schottky barrier silicon diodes were used to provide additional discharge paths to the Geiger charge developed across the ?APD junction (Figure 7b). SMT components helped to minimize the parasitic effects: these elements are schematically depicted in Figure 7c.
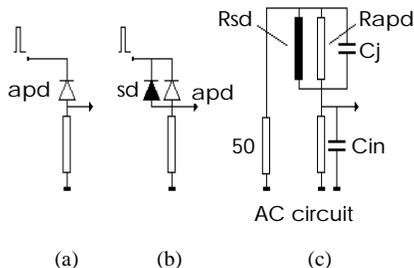

Figure 7(a): Schematic of the pulsed bias with resistive load; (b) Schottky diode (sd) connected in parallel with the ?APD sinks more charge to ground during the charge recovery period (pulsed bias OFF); (c) Equivalent *ac* circuit, showing the parasitic elements of the

components and the 50 ? internal resistance of the pulse generator. SMT components were used to minimize the stray impedance of the circuit.

This improved pulsed bias circuit was tested for the Geiger reset time and the results are shown in Figure 8. The pulsed quenching circuit results in 25 nsec quenching time and 75 nsec reset time. Further improvements are required to decrease the reset time and optimize the circuit.
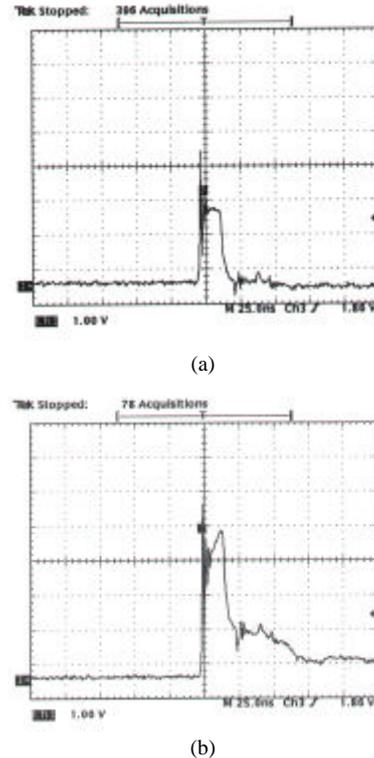

(a)

(b)

Figure 8: Pulses bias active quenching with the circuit described in Figure 7(b): (a) The ?APD is biased above the breakdown voltage and the charging signal is collected on the limiting resistor (no Geiger event occurs); (b) Geiger pulses, are registered in ?APD and are quenched within 25nsec.

IV. PULSE AMPLITUDE SPECTRA

A typical Geiger pulse amplitude spectrum, generated by single electrons in ?APD pixels, is shown in Figure 9. The Geiger avalanche was quenched using 100 K? limiting series resistors (passive quenching) and the corresponding gain was in the 10^8-10^9 range. No baseline noise is present in the Geiger pulse spectrum. This is to be compared to PMTs, where accurate threshold setting is required to avoid excessive noise pick-up (threshold too low) or signal loss (threshold too high). The Geiger pulse spectrum in ?APDs does not require accurate threshold control and consequently the long term pulse stability requirement can be relaxed. This is of paramount importance for large array calibration, and for long-term servicing in multi-layered detector structures encountered in modern accelerator experiments.
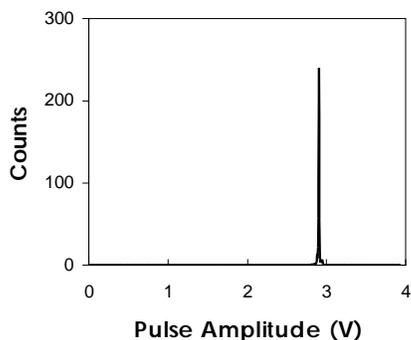
Figure 9: Single photon generated pulse height amplitude spectrum of Geiger mode operated ?APDs, biased at 3 volts above the breakdown voltage. The avalanche is passively quenched with 100 K? limiting resistors. Assuming the avalanche is triggered by single carriers, the multiplied charge corresponds to a charge gain of 5 x 10^8. The narrow peak (FWHM = 0.3%) demonstrates uniform avalanche multiplication across the ?APD sensitive area.

Figure 10 presents the Geiger pulse spectrum for pulsed bias quenching. The first peak represents the charging current pulses (baseline pulses) while the second peak represents the Geiger charge riding on the baseline pulse. The pulse separation is proportional to the Geiger charge generated during the short time the ?APD was biased in Geiger mode. As compared to the spectra acquired in passive quenching, where the baseline noise can be practically ignored (Figure 9), the pulsed quenching spectra would require discriminators to reject the lower amplitude baseline pulses (noise). However, the clear separation of the baseline noise would not require tight control of the threshold level.
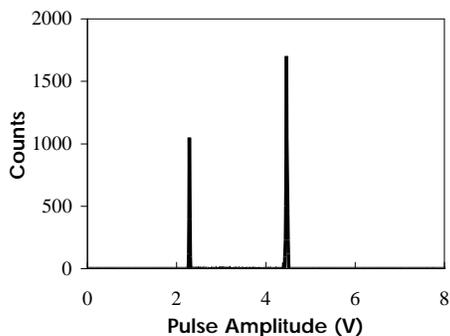

Figure 10: Pulse height amplitude spectrum of Geiger mode operated ?APDs, operated with pulsed bias above the breakdown voltage. The first peak (left) is due to the charging current only (no Geiger events), while the second peak is due to Geiger and charging currents through ?APD.

V. SUMMARY

High gain APD arrays were designed and developed for Cherenkov radiation imaging. The prototype array will have 84 pixel Geiger mode operated ?APDs and efficient micro-concentrator arrays. The ?APD array exhibits gains higher than 10^8, can reach 25 nsec quench time and 75 nsec reset time when actively quenched. When used with a focusing mirror and micro-concentrator mirror arrays in direct contact with the ?APDs, a fill factor close to 100% and 70% light focusing efficiency could be achieved. The resulting unit holds promise of a compact, high detection efficiency array for spatial imaging of extremely low intensity Cherenkov events.

VI. ACKNOWLEDGMENTS

VII. REFERENCES

[1] BaBar Technical Design Report, SLAC-R-95-457, March 1995.
[2] S. Vasile, P. Gothoskar, R. Farrell and D. Sdrulla, "Photon detection with high gain avalanche photodiode arrays," IEEE Trans. Nucl.Sci., vol 45, no 3, pp. 720-723, 1998.
[3] T. Kamae, H. Arai, T. Ohtsuka, N. Tsuchida, H. Aihara "Focussing DIRC – A new compact Cherenkov ring imaging device," Nucl. Instrum. Meth. A382, pp. 430-440, 1996.
[4] R.G.W.Brown, R.Jones, J.R.Rarity, K.D.Ridley, "Characterization of silicon avalanche photodiodes for photon correlation measurements. 2: Active quenching," Applied Optics, Vol. 26, no 12, pp. 2383-2388, 1987.
[5] A.W.Lightstone, R.J.McIntyre, "Photon counting silicon avalanche photodiodes for photon correlation spectroscopy," OSA Proceedings on Photon Correlation Techniques and Applications, OSA , Vol. 1, Washington D.C. pp. 183-191, 1988.
[6] H.Dautet, P.Deschamps, B.Dion, A.D. McGregor et. al. "Photon counting techniques with silicon avalanche photodiodes," Applied Optics, Vol. 32, no 21, pp. 3894-3900, July 1993.
[7] R.Marino, J.R.Ochoa, A.Sanchez, S.DiCecca, N.R.Newburry, S.Vasile, "3D Imaging laser radar with photonic sensitivity," Proc. IRIS Systems, May, 1996.
[8] S. Vasile, J. Gordon, R. Farrell, M. Squillante and G. Entine, "Fast avalanche photodiode detectors for scintillating fibers," Workshop on Scintillating Fiber Detectors, Notre Dame IN, Eds. A. D. Bross et al., World Scientific, 1993, pp. 653-660.
[9] H. Fenker, T. Regan, J. Thomas, M. Wright (SSCL), "Higher efficiency active circuit for avalanche photodiodes," SSCL-PREPRINT-458, Jun 1993.